

## Photoelectrochemical cell using dye sensitized zinc oxide nanowires grown on carbon fibers

Husnu Emrah Unalan,<sup>1,a)</sup> Di Wei,<sup>2</sup> Kenichi Suzuki,<sup>3</sup> Sharvari Dalal,<sup>1</sup> Pritesh Hiralal,<sup>1</sup> Hidetoshi Matsumoto,<sup>3</sup> Shinji Imaizumi,<sup>3</sup> Mie Minagawa,<sup>3</sup> Akihiko Tanioka,<sup>3</sup> Andrew J. Flewitt,<sup>1</sup> William I. Milne,<sup>1</sup> and Gehan A. J. Amaratunga<sup>1</sup>

<sup>1</sup>*Department of Engineering, University of Cambridge, 9 JJ Thomson Avenue, Cambridge CB3 0FA, United Kingdom*

<sup>2</sup>*Nokia Research Centre, 11 JJ Thomson Avenue, Cambridge CB3 0FF, United Kingdom*

<sup>3</sup>*Department of Organic and Polymeric Materials, Tokyo Institute of Technology, Tokyo 152-8552, Japan*

(Received 12 June 2008; accepted 17 August 2008; published online 3 October 2008)

Zinc oxide (ZnO) nanowires (NWs) grown on carbon fibers using a vapor transport and condensation approach are used as the cathode of a photoelectrochemical cell. The carbon fibers were obtained by electrospray deposition and take the form of a flexible carbon fabric. The ZnO NW on carbon fiber anode is combined with a “black dye” photoabsorber, an electrolyte, and a platinum (Pt) counterelectrode to complete the cell. The results show that ZnO NW and carbon fibers can be used for photoinduced charge separation/charge transport and current collection, respectively, in a photoelectrochemical cell. © 2008 American Institute of Physics. [DOI: 10.1063/1.2978957]

Dye sensitized solar cells (DSSCs) hold promise for photovoltaic energy generation/harvesting.<sup>1–5</sup> Their lower cost, high efficiency (compared to other nonsilicon alternatives), environmental friendliness, and low angle dependency on the incident light are some factors, which make them attractive for deployment in environments for which conventional silicon cells are either commercially or physically unviable. The conversion efficiency of liquid electrolyte DSSCs utilizing fluorine doped tin oxide coated glass substrates as anode material has been currently improved to above 11% (100 mW/cm<sup>2</sup>).<sup>6</sup> However, if DSSCs could be flexible then they can be used in various applications, for example as “stick on” power sources for electronics embedded into clothing. Current studies on flexible DSSCs utilize indium tin oxide coated polyethylene terephthalate substrates as a transparent anode material.<sup>7,8</sup> The use of a polymer substrate imposes a temperature limit, which is well below the optimum sintering temperature of the dye absorbing nanoparticles, limiting the efficiency of the cells (lower than 2.3%). Kang *et al.*<sup>9</sup> reported a flexible DSSC utilizing metallic supporting substrate. A flexible stainless steel anode with the advantage of high temperature sinterability yielded photovoltaic efficiency of 4.2%. Recently, stainless steel wires<sup>10</sup> and meshes<sup>11</sup> have been used to fabricate DSSCs signifying the necessity of high temperature processable electrode materials for high performance flexible DSSCs.

Commonly used anode materials for DSSCs include nanoparticles or thin films of titanium dioxide (TiO<sub>2</sub>), tin dioxide (SnO<sub>2</sub>), and zinc oxide (ZnO) that are deposited as a paste, and then sintered for electrical continuity. Reported efficiency values for nanoparticles are still higher than for thin films. Nanoparticle films enable large internal surface area for the attachment of dye molecules and provide percolation pathways for electrons. In order to improve DSSC efficiency, Law *et al.*<sup>12</sup> replaced the nanoparticle film with an array of oriented single crystalline nanowires (NWs) and the

necessity of higher dye loadings through an increase in the electrode surface area has been clearly identified. We expand on this approach by providing a three-dimensional (3D) surface for ZnO NW growth, thereby further increasing electrode surface area.

In this work, we have synthesized highly conductive and flexible carbon fiber mat through a simple electrospray deposition (ESD) procedure and conformably grown single crystalline ZnO NWs on the individual fibers through chemical vapor deposition (CVD). Following the attachment of dye molecules, the performance of this 3D anode was combined with a lithium iodide/iodine (Li-I/I<sub>2</sub>) electrolyte and a Pt counterelectrode to complete the cell.

Carbon fibers were synthesized as reported elsewhere.<sup>13</sup> Briefly, methanol solutions of phenolic resin and poly(vinyl butyral) was injected through a stainless steel nozzle with an applied voltage of 15 kV. Depositions were carried out at ambient conditions, and fibers were collected on a grounded aluminum collector. The as-deposited fibers were then cured by adding formaldehyde followed by carbonization. ZnO NWs were grown on carbon fibers by the carbothermal reduction of ZnO powder at 1020 °C, as described in detail elsewhere.<sup>14</sup> The original black carbon fibers turned bluish-white in color, indicating growth of significant amount of ZnO NWs on the carbon fibers. 10 and 30 min growth resulted in 1 and 5 μm long NWs, respectively. NWs were grown in an area of 3×3 mm<sup>2</sup> area, which will, in turn, determine the device area. The best dye sensitizer reported to date is tris(isothiocyanato)-ruthenium(II)-2,2';6',2''-terpyridine-4,4',4''-tricarboxylic acid, tris-tetrabutylammonium salt (so called “black dye”) with visible absorption extending to the near infrared region up to 920 nm.<sup>15</sup> The carbon fiber ZnO NW composites were then immersed into a solution of 0.5 mM black dye in ethanol overnight. Photoelectrochemical measurements were conducted under ambient conditions using a Pt (99.9%) foil as a counterelectrode. Pt foil was placed 1 cm away from the composite. Acetonitrile solution containing 0.1M LiI and 0.05M I<sub>2</sub> was used as the electrolyte. An Oriel 450W xenon

<sup>a)</sup>Author to whom correspondence should be addressed. Electronic mail: heu22@cam.ac.uk.

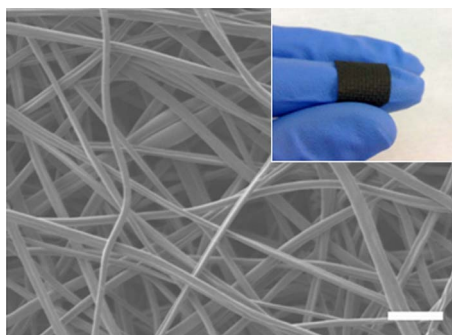


FIG. 1. (Color online) SEM image of the carbonized carbon fiber fabric with an average diameter of  $1.16 \mu\text{m}$ . Scale mark corresponds to  $10 \mu\text{m}$ . The inset shows a photograph of the flexible fiber.

arc lamp with an AM1.5 filter was used as an excitation source. A HP 4140B semiconductor analyzer was used to measure current-voltage ( $I$ - $V$ ) characteristics. The photoluminescence (PL) measurements were performed at room temperature with the 266 nm line of a Nd:yttrium aluminum garnet laser. The morphology of the synthesized materials were investigated using the scanning electron microscopy (SEM) (JEOL 6340F, operated at 5 kV). X-ray diffraction (XRD) patterns were taken with a Philips PW1730 diffractometer ( $\text{Cu } K\alpha$  radiation  $1.54060 \text{ \AA}$ ). High resolution transmission electron microscopy (HRTEM) was performed on a JEOL 3011 operated at 300 kV. The HRTEM samples were prepared by dispersing NWs by sonication in isopropanol and placing them onto holey carbon grids.

A SEM image of the carbon fibers following carbonization is shown in Fig. 1. The average diameter of the fibers was measured to be  $1.16 \mu\text{m}$ . A photograph of the carbon fibers following the carbonization treatment is shown in the inset, as deposited phenolic resin fabrics cannot maintain their shape during the heat treatment. Therefore, a curing step by formaldehyde prior to carbonization was found to be crucial for dimensional stability and flexibility.

Figure 2(a) shows the SEM image of the ZnO NWs grown on the carbon fibers. The NWs are approximately  $5 \mu\text{m}$  in length as shown in Fig. 2(a) and about  $50 \text{ nm}$  in diameter as shown in Fig. 2(b). Complete surface coverage of the carbon fibers by ZnO NWs can be clearly seen. The highly crystalline nature of the ZnO NWs grown on carbon fibers is indicated by the measured XRD pattern, shown in Fig. 2(c). There is no specific orientation for the ZnO NWs since they are grown conformally on the circumference of the carbon fibers. The diffraction patterns were indexed to a typical hexagonal wurtzite structure of bulk ZnO with unit cell constants of  $a=3.252 \text{ \AA}$  and  $c=5.213 \text{ \AA}$ . Crystallinity of the wires was further confirmed by transmission electron microscopy (TEM) analysis, see Fig. 2(b). The selected area electron diffraction (SAED) pattern shows that the NWs are single crystalline with the  $[0001]$  growth direction (inset). The optical quality of the ZnO NWs was investigated by PL. Figure 2(d) shows the PL spectra taken from ZnO NWs grown on carbon fibers. A strong luminescence peak is seen at  $378 \text{ nm}$ , corresponding to the near band gap emission responsible for the recombination of free excitons in ZnO.<sup>16</sup> The full width half maximum (FWHM) value of the primary luminescence peak is  $13 \text{ nm}$ . A low FWHM value for the strong ultraviolet peak coupled with the absence of defect

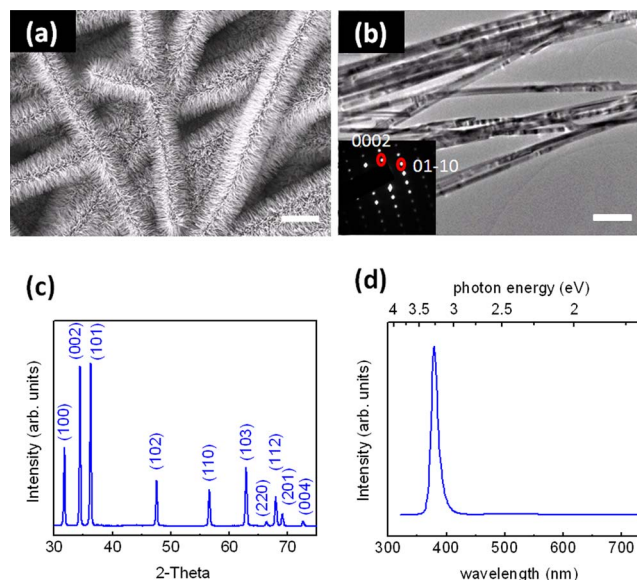


FIG. 2. (Color online) (a) SEM and (b) TEM images of the ZnO NWs grown on carbon fibers by CVD process. The inset shows the SAED pattern from the NWs indicating the single crystalline nature with  $[0001]$  growth direction. Scale marks correspond to  $10 \mu\text{m}$  and  $500 \text{ nm}$ , respectively. (c) XRD pattern and (d) PL spectrum obtained from the composite.

related broad green peak indicates the defect-free nature of the synthesized NWs.

In Fig. 3(a),  $I$ - $V$  curves of the composites with different NW lengths obtained from photoelectrochemical measurements are shown. Measurements were made under  $100 \text{ mW/cm}^2$  (AM1.5) illumination and in the dark following the attachment of black dye molecules. The figure indicates the importance of the length of the NWs. For the composite with  $1 \mu\text{m}$  ZnO NWs, measured open circuit voltage ( $V_{oc}$ ), short circuit current density ( $J_{sc}$ ), and fill factor were

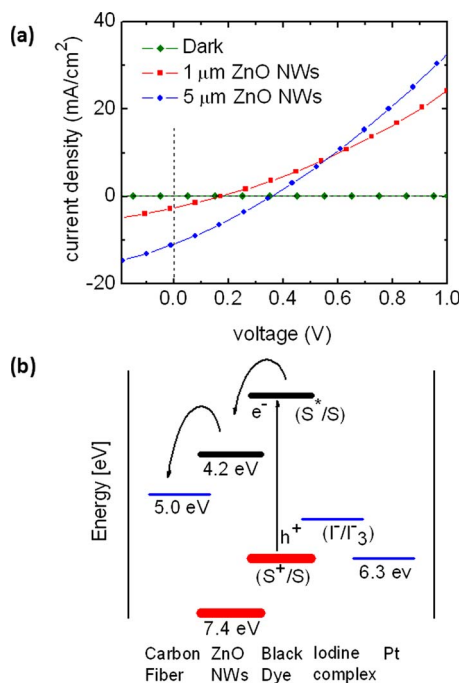


FIG. 3. (Color online) (a)  $I$ - $V$  characteristics under no illumination and under one sun ( $100 \text{ mW/cm}^2$ ) obtained during photoelectrochemical measurements using both  $1$  and  $5 \mu\text{m}$  long ZnO NWs. (b) Energy level diagram with respect to vacuum level for the photoelectrochemical setup.

170 mV, 2.6 mA/cm<sup>2</sup>, and 0.25, respectively. The corresponding values for the composite with 5 μm ZnO NWs were 350 mV, 11.2 mA/cm<sup>2</sup>, and 0.28, respectively. Both  $V_{oc}$  and  $J_{sc}$  were found to increase with NW length. Higher  $J_{sc}$  can be attributed to the amount of dye molecules that can be attached to the NWs. The relatively low  $V_{oc}$  in both cells is an indication of excessive recombination, most likely at the dye/ZnO NW interface. The true diode potential of the photocells is indicated by the crossover voltage of the two *IV* characteristics ~0.6 V. ZnO NW layer not only affect the dye's adsorption but also influences the kinetic behavior of the carriers. Due to the 3D nature of the electrode, incident light cannot leave the electrode simply through direct penetration. It is dispersed through the entire working electrode. The longer ZnO NWs increase the scattering of the light inside the electrode, whereas for shorter ZnO NWs scattering is too weak. Therefore for shorter NWs, dark side of the electrode is in a poor working state, which reduces the short circuit current. This means the photocurrent goes to zero before the "true" energy level related open circuit voltage is reached. When the light scattering is increased with the longer NWs, there is more absorption by the dye molecules and a higher photocurrent. Thus, external terminal current goes to zero at higher voltages.

Recombination is evident in the low value of the shunt resistance in the system. At low shunt resistances, the voltage from the solar cell is reduced. *IV* curves given in Fig. 3(a) reveal the value of the parallel/shunt resistances [ $R_{sh} = (dV/dI)_{V=0}$ ] being  $R_{sh} = 74 \Omega \text{ cm}^2$  for 1 μm long ZnO NWs and  $R_{sh} = 43.3 \Omega \text{ cm}^2$  for 5 μm ones.<sup>17</sup> The growth of ZnO NWs on carbon fibers is a self-catalytic process. Annealing carbon fibers in the presence of oxygen with the purpose of recovering ZnO NWs<sup>18</sup> revealed the presence of a ZnO underlying layer. These shunt resistances are due to the ZnO underlayer that forms on the circumference of the carbon fibers at the bottom of the ZnO NWs. In fact, this underlayer is mutually beneficial. It also prevents the penetration of electrolyte to the carbon fiber.<sup>19</sup> Shorter ZnO NWs have a thinner underlayer, whereas longer NWs yield a thicker one. Thinner underlayer may allow the penetration of electrolyte into the carbon fiber, which would consecutively yield to the photoshunt and lower  $V_{oc}$ .

The charge transfer and transport in the photoelectrochemical cell can be understood from the energy diagram shown in Fig. 3(b). Upon irradiation, excitons are generated in the black dye, separated in the NW interface. Electron transfer is achieved through the NWs followed by the carbon fibers. Holes, on the other hand, are transferred through the iodine electrolyte and collected in the Pt electrode.

Catalyst-free growth of ZnO NWs at high temperatures on carbon flakes<sup>18</sup> and carbon cloth<sup>20</sup> has been already demonstrated. In this work, smaller diameter ESD deposited flexible carbon fibers were used as the template for the NW growth. Carbon fibers retained their flexibility and conductivity after the growth of ZnO NWs. Each ZnO NW is in direct contact with the conducting carbon fiber for improved charge transfer. Electron transfer through these highly crystalline NWs is expected to be faster than the percolation through the conventionally used TiO<sub>2</sub> particles. This dense

3D NW network enables high dye loading, which would lead to an efficient exciton generation under illumination. The results indicate that the ZnO NW dye interface should be passivated to improve performance. We have assumed a two-dimensional area for the measurements; however, due to the 3D nature of the electrode, the actual device area could be orders of magnitude higher. In fact, the high  $J_{sc}$  obtained from the experiments can be attributed to that. This electrode material combines the flexibility of the fibers with the light weight nature of the carbon. It should be noted that the aim here is not to fabricate state-of-the-art DSSCs. Instead, the objective is to demonstrate the use of carbon fiber ZnO NW composite as a flexible anode material.

In summary, we have demonstrated that highly crystalline ZnO NWs can be grown on ESD deposited carbon fibers at high temperatures, and this composite can be used as an anode material for the fabrication of flexible DSSCs. The prepared carbon fiber NW heterojunctions are promising for various potential applications, including wearable electronic and photonic devices.

This work was funded through the Nokia–Cambridge University Strategic Research Alliance in Nanotechnology.

- <sup>1</sup>B. O'Regan and M. Grätzel, *Nature (London)* **353**, 737 (1991).
- <sup>2</sup>M. K. Nazeeruddin, A. Kay, I. Rodicio, R. Humphry-Baker, E. Müller, P. Liska, N. Vlachopoulos, and M. Grätzel, *J. Am. Chem. Soc.* **115**, 6382 (1993).
- <sup>3</sup>U. Bach, D. Lupo, P. Comte, J. E. Moser, F. Weissortel, J. Salbeck, H. Spreitzer, and M. Grätzel, *Nature (London)* **395**, 583 (1998).
- <sup>4</sup>P. Wang, C. Klein, R. Humphry-Baker, S. M. Zakeeruddin, and M. Grätzel, *Appl. Phys. Lett.* **86**, 123508 (2005).
- <sup>5</sup>S. Ito, S. M. Zakeeruddin, R. Humphry-Baker, P. Liska, R. Charvet, P. Comte, M. K. Nazeeruddin, P. Pechy, M. Takata, H. Miura, S. Uchida, and M. Grätzel, *Adv. Mater. (Weinheim, Ger.)* **18**, 1202 (2006).
- <sup>6</sup>M. K. Nazeeruddin, F. D. Angelis, S. Fantacci, A. Selloni, G. Viscardi, P. Liska, S. Ito, B. Takeru, and M. Grätzel, *J. Am. Chem. Soc.* **127**, 16835 (2005).
- <sup>7</sup>S. Uchida, M. Tomiha, H. Takizawa, and M. Kawaraya, *Sol. Energy Mater. Sol. Cells* **81**, 135 (2004).
- <sup>8</sup>M. Durr, A. Schmid, M. Obermaier, S. Rosselli, A. Yasuda, and G. Nelles, *Nat. Mater.* **4**, 607 (2005).
- <sup>9</sup>M. G. Kang, N. G. Park, K. S. Ryu, S. H. Chang, and K. J. Kim, *Sol. Energy Mater. Sol. Cells* **90**, 574 (2006).
- <sup>10</sup>X. Fan, Z. Chu, F. Wang, C. Zhang, L. Chen, Y. Tang, and D. Zou, *Adv. Mater. (Weinheim, Ger.)* **20**, 592 (2008).
- <sup>11</sup>X. Fan, F. Wang, Z. Chu, L. Chen, C. Zhang, and D. Zou, *Appl. Phys. Lett.* **90**, 073501 (2007).
- <sup>12</sup>M. Law, L. E. Greene, J. C. Johnson, R. Saykally, and P. Yang, *Nat. Mater.* **4**, 455 (2005).
- <sup>13</sup>K. Suzuki, H. Matsumoto, M. Minagawa, M. Kimura, and A. Tanioka, *Polym. J. (Tokyo, Jpn.)* **39**, 1128 (2007).
- <sup>14</sup>S. H. Dalal, D. L. Baptista, K. B. K. Teo, R. G. Lacerda, D. A. Jefferson, and W. I. Milne, *Nanotechnology* **17**, 4811 (2006).
- <sup>15</sup>Z. S. Wang, T. Yamaguchi, H. Sugihara, and H. Arakawa, *Langmuir* **21**, 4272 (2005).
- <sup>16</sup>Y. C. Kong, D. P. Yu, B. Zhang, W. Fang, and S. Q. Feng, *Appl. Phys. Lett.* **78**, 407 (2001).
- <sup>17</sup>J. B. Baxter and E. S. Aydil, *Appl. Phys. Lett.* **86**, 053114 (2005).
- <sup>18</sup>D. Banerjee, J. Y. Lao, D. Z. Wang, J. Y. Huang, D. Steeves, B. Kimball, and Z. F. Ren, *Nanotechnology* **15**, 404 (2004).
- <sup>19</sup>J. B. Baxter, A. M. Walker, K. van Ommering, and E. S. Aydil, *Nanotechnology* **17**, S304 (2006).
- <sup>20</sup>D. Banerjee, S. H. Jo, and Z. F. Ren, *Adv. Mater. (Weinheim, Ger.)* **16**, 2028 (2004).

Applied Physics Letters is copyrighted by the American Institute of Physics (AIP). Redistribution of journal material is subject to the AIP online journal license and/or AIP copyright. For more information, see <http://ojps.aip.org/aplo/aplcr.jsp>